algorithms

MDPI

Article

The Nonlinear Relationship Between Fasting Plasma Glucose, HbA1c, and Blood Pressure: A Cross-Sectional Analysis of 54,881 Adults from NHANES 1999–2023

Mikhail Kolev [1,2,*], Irina Naskinova [1], Mariyan Milev [1,3,*], Hristo Kalinov [4], Gabriela Vasileva [5] and Penko Mitev [6]

[1] Department of Mathematics, University of Architecture, Civil Engineering and Geodesy, 1 Hristo Smirnenski Blvd., 1164 Sofia, Bulgaria; inaskinova_fte@uacg.bg
[2] Faculty of Fire Safety and Civil Protection, Academy of the Ministry of Interior, 170 Pirotska Str., 1309 Sofia, Bulgaria
[3] Department of Statistics and Econometrics, Faculty of Economics and Business Administration, Sofia University "St. Kliment Ohridski", 125 Tsarigradsko Shosse Blvd., bl. 3, 1113 Sofia, Bulgaria
[4] Faculty of Mathematics and Informatics, Sofia University "St. Kliment Ohridski", 5 James Boucher Blvd., 1164 Sofia, Bulgaria; hkalinov@uni-sofia.bg
[5] Faculty of Social Business and Computer Sciences, Varna Free University, Chayka Resort, 9007 Varna, Bulgaria; gabivassi@gmail.com
[6] Faculty of Mechanical Engineering, Mechanical and Instrument Engineering, Technical University of Sofia, Branch Plovdiv, 4000 Plovdiv, Bulgaria; penkomitev@tu-plovdiv.bg
* Correspondence: mkolev_fte@uacg.bg (M.K.); m.milev@feb.uni-sofia.bg (M.M.)

Abstract

The relationship between blood glucose levels and blood pressure is well established in clinical literature, yet its precise quantitative characterization, including nonlinear effects, threshold phenomena, and demographic modifiers, remains incompletely understood. In this study, we conducted a comprehensive cross-sectional analysis of the National Health and Nutrition Examination Survey (NHANES) spanning 11 survey cycles (1999–2023), comprising 54,881 adult participants with at least one glycemic marker and standardized blood pressure measurements. Of these, 26,981 had valid fasting plasma glucose (FPG) measurements, and 49,327 had valid glycated hemoglobin (HbA1c) measurements. We employed restricted cubic splines (RCS), generalized additive models (GAMs), and segmented regression to characterize the dose–response relationship between glycemic markers and both systolic (SBP) and diastolic blood pressure (DBP). A 10 mg/dL increase in FPG was associated with a 0.32 mmHg increase in SBP (95% CI: 0.26–0.38, $p < 0.001$) after adjusting for age, sex, and body mass index (BMI). Nonlinearity was statistically significant for all exposure–outcome combinations ($p < 10^{-7}$ for Wald tests). Segmented regression identified a FPG breakpoint at 122.1 mg/dL (95% CI: 119.5–125.6), below which SBP increased at 0.39 mmHg per mg/dL and above which the association was essentially flat. Stratified analyses revealed that the glucose–BP association was strongest in females ($\beta = 0.048$ per mg/dL) compared with males ($\beta = 0.021$), and in prediabetic individuals ($\beta = 0.065$) compared with those with established diabetes ($\beta = 0.014$). In the statistical mediation decomposition, body mass index accounted for 23.5% of the total FPG–SBP association. A significant FPG $\times$ BMI interaction ($p < 0.001$) indicated that the glucose–BP relationship is modulated by adiposity. These findings provide a large-scale population-level analysis of the glucose–blood pressure dose–response relationship and identify potential thresholds warranting further investigation for integrated cardiometabolic risk management (95% bootstrap CI: 19.3–28.9%; 1000 resamples); given the cross-sectional design and BMI's plausible role as a shared upstream determinant of glucose and blood pressure, this proportion is reported as a confounding decomposition rather than as evidence of causal mediation. Insulin

Check for updates

Academic Editor: Micheal Olaolu Arowolo

Received: 23 March 2026
Revised: 30 April 2026
Accepted: 1 May 2026
Published: 7 May 2026

Copyright: © 2026 by the authors. Licensee MDPI, Basel, Switzerland. This article is an open access article distributed under the terms and conditions of the Creative Commons Attribution (CC BY) license.

resistance (HOMA-IR) and C-reactive protein did not contribute significantly as additional decomposition pathways.

Keywords: blood glucose; blood pressure; NHANES; nonlinear relationship; restricted cubic splines; generalized additive models; mediation analysis; cardiometabolic risk; dose–response; fasting plasma glucose; HbA1c; hypertension

1. Introduction

Hypertension and hyperglycemia represent two of the most prevalent cardiometabolic risk factors globally, affecting approximately 1.28 billion and 537 million adults, respectively [1,2]. Their co-occurrence is strikingly common: 40–60% of individuals with type 2 diabetes mellitus (T2DM) also have hypertension, and the combination dramatically amplifies the risk of cardiovascular disease, stroke, chronic kidney disease, and all-cause mortality [3,4]. Understanding the precise quantitative relationship between blood glucose levels and blood pressure is therefore essential for optimizing cardiometabolic risk stratification and guiding therapeutic decision-making.

Several pathophysiological mechanisms have been proposed to link hyperglycemia with elevated blood pressure. Chronic hyperinsulinemia, a hallmark of insulin resistance, promotes renal sodium retention through enhanced activity of the epithelial sodium channel (ENaC) and stimulation of the sympathetic nervous system [5]. Hyperglycemia directly impairs endothelial function by reducing nitric oxide bioavailability through increased oxidative stress and advanced glycation end-product (AGE) formation [6]. Additionally, activation of the renin–angiotensin–aldosterone system (RAAS) in the setting of metabolic syndrome further contributes to vascular stiffness and hypertension [7]. Despite these well-characterized pathways, the dose–response relationship between glycemic markers and blood pressure at the population level remains poorly quantified.

Prior epidemiological studies have generally assumed a linear association between fasting plasma glucose (FPG) or glycated hemoglobin (HbA1c) and blood pressure, yet emerging evidence suggests that this relationship may be nonlinear, with acceleration above certain glycemic thresholds [8,9]. Furthermore, the extent to which demographic factors such as age, sex, body mass index (BMI), and antihypertensive medication use modify this association has not been systematically evaluated in a large, nationally representative cohort. Similarly, the relative contributions of insulin resistance, adiposity, and systemic inflammation as mediators of the glucose–blood pressure link have not been quantified in a unified analytical framework.

The National Health and Nutrition Examination Survey (NHANES) provides a unique opportunity to address these gaps, as it collects standardized measurements of fasting glucose, HbA1c, blood pressure, anthropometry, insulin, and inflammatory biomarkers in a large, nationally representative sample of the United States civilian non-institutionalized population. By pooling data across 11 survey cycles spanning 24 years (1999–2023), we can achieve sufficient statistical power to detect nonlinear effects, identify subgroup heterogeneity, and decompose mediation pathways.

The present study advances the field in several ways. First, we characterize the dose–response relationship between FPG/HbA1c and SBP/DBP using restricted cubic splines, generalized additive models, and segmented regression, providing formal statistical tests for nonlinearity. Second, we identify a data-driven FPG breakpoint above which the glucose–BP association changes slope. Third, we quantify effect modification by age, sex, BMI, diabetes status, and antihypertensive medication use through stratified analyses and

formal interaction testing. Fourth, we apply a statistical decomposition of the marginal FPG–SBP association into pathways involving adiposity (BMI), insulin resistance (HOMA-IR), and inflammation (C-reactive protein); because BMI plausibly acts as an upstream confounder rather than a downstream mediator on cross-sectional data, this is presented as a confounding decomposition with bootstrap-derived confidence intervals rather than causal mediation. Finally, we examine whether the glucose–BP association has shifted over 24 years of evolving treatment patterns and lifestyle changes.

2. Materials and Methods

2.1. Data Source and Study Population

We used data from the NHANES, a series of cross-sectional surveys conducted by the National Center for Health Statistics (NCHS) of the Centers for Disease Control and Prevention (CDC). NHANES employs a complex, multistage probability sampling design to obtain a nationally representative sample of the United States civilian non-institutionalized population. Each survey cycle includes a household interview and a standardized health examination at a mobile examination center (MEC). We pooled data from 11 continuous NHANES cycles: 1999–2000, 2001–2002, 2003–2004, 2005–2006, 2007–2008, 2009–2010, 2011–2012, 2013–2014, 2015–2016, 2017–2018, and 2021–2023. The 2017–March 2020 pre-pandemic cycle was excluded to avoid overlap with the 2017–2018 cycle.

From an initial pool of 113,249 participants across all cycles, we restricted the sample to adults aged 18–80 years (n = 65,732), further requiring valid blood pressure measurements (n = 58,014) and at least one glycemic measure (FPG or HbA1c; n = 55,386). We excluded participants with physiologically implausible values for FPG (<40 or >600 mg/dL), HbA1c (<3.0% or >18.0%), SBP (<70 or >250 mmHg), DBP (<30 or >150 mmHg), or BMI (<12 or >70 kg/m^2). The final analytic sample comprised 54,881 participants. Figure 1 presents the study population selection flowchart.

Reading Figure 1 from top to bottom traces the impact of each selection rule on the analytic sample. The largest single attrition step is the age restriction to adults 18–80 years (47,517 participants excluded, predominantly children and adolescents in NHANES MEC examinations), followed by the requirement for at least one valid blood-pressure reading (7718 excluded) and the requirement for at least one valid glycaemic measure—FPG or HbA1c—(2628 excluded). Application of physiological-plausibility filters on FPG, HbA1c, SBP, DBP, and BMI removed a further 505 participants. The resulting 54,881-participant cohort retains 48.5% of the original 113,249 NHANES respondents and is the population to which all subsequent analyses refer; the FPG-validated subsample (n = 26,981, used in Tables 1 and 2 and the segmented regression) is approximately half of this cohort, reflecting the fact that FPG is collected only in the morning fasting subsample, whereas HbA1c is collected in all examined participants.

To clarify the analytic samples used throughout, the full sample of 54,881 participants with at least one glycemic measure (FPG or HbA1c) was used for HbA1c-based analyses. FPG-specific analyses (including Table 1, dose–response modeling, segmented regression, stratified analyses, and mediation) used the fasting subsample of 26,981 participants with valid FPG measurements and appropriate fasting subsample weights (WTSAF2YR). HOMA-IR–based analyses were further restricted to participants with valid insulin measurements ($n \approx$ 22,400).

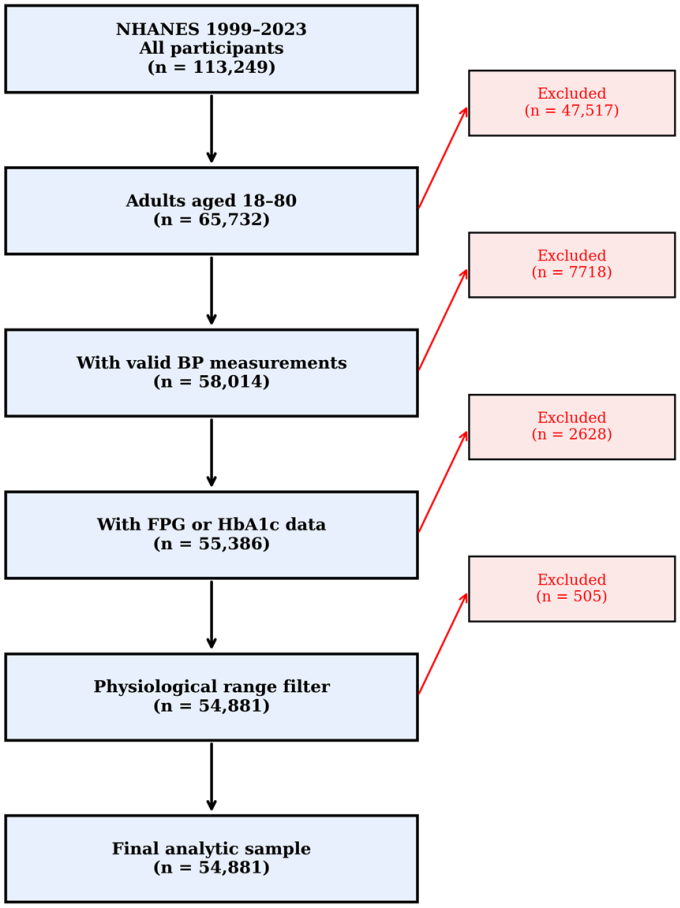


Figure 1. CONSORT-style study population selection flowchart showing sequential application of exclusion criteria to the pooled NHANES 1999–2023 dataset. Blue boxes (left column) indicate the number of participants retained at each stage; red boxes (right column) indicate the number excluded at each step with the corresponding reason. Starting from 113,249 total NHANES participants, sequential exclusions for age (adults 18–80 only), valid blood pressure measurement availability, glycemic data completeness (FPG or HbA1c), and physiological range plausibility yielded a final analytic sample of 54,881 adults. Black downward arrows connect successive inclusion stages.

Table 1. Baseline characteristics of the study population by fasting plasma glucose category (n = 26,981 with valid FPG). Values for continuous variables are presented as mean ± SD; categorical variables are presented as n (%). FPG = fasting plasma glucose; BMI = body mass index; HOMA-IR = homeostatic model assessment of insulin resistance; CRP = C-reactive protein; SBP = systolic blood pressure; DBP = diastolic blood pressure. p-values from Kruskal–Wallis test (continuous) or chi-squared test (categorical).

≥200	126–199	110–125	100–109	<100	Variable
785	2369	3371	6473	13,983	n
54.3 ± 14.2	59.8 ± 13.5	54.9 ± 15.4	48.3 ± 16.4	41.0 ± 16.1	Age (years)
43.90%	43.90%	41.70%	44.10%	58.80%	Female (%)
32.7 ± 7.3	32.6 ± 7.5	31.3 ± 7.0	29.4 ± 6.4	27.1 ± 6.0	BMI (kg/m^2)
269.1 ± 63.2	147.9 ± 19.7	115.4 ± 4.4	103.9 ± 2.8	91.1 ± 6.2	FPG (mg/dL)
9.7 ± 1.9	6.8 ± 1.1	5.7 ± 0.5	5.5 ± 0.4	5.3 ± 0.4	HbA1c (%)
17.4 ± 23.2	9.0 ± 14.0	5.0 ± 4.3	3.4 ± 3.0	2.2 ± 2.3	HOMA-IR
3.2 ± 6.0	3.2 ± 8.1	2.9 ± 6.8	1.9 ± 4.4	1.4 ± 4.3	CRP (mg/L)
129.8 ± 19.0	129.6 ± 18.8	127.0 ± 17.8	122.5 ± 16.2	117.1 ± 15.7	SBP (mmHg)
73.9 ± 12.0	71.4 ± 11.9	72.4 ± 11.7	72.2 ± 11.4	69.8 ± 10.8	DBP (mmHg)

Table 2. Mean systolic and diastolic blood pressure by fasting plasma glucose category (n = 26,981 with valid FPG). Values are presented as unweighted mean ± standard deviation. FPG categories follow American Diabetes Association thresholds: <100 mg/dL (normal), 100–109 mg/dL (low-risk prediabetes), 110–125 mg/dL (high-risk prediabetes), 126–199 mg/dL (diabetes), ≥200 mg/dL (severe hyperglycemia). SBP = systolic blood pressure; DBP = diastolic blood pressure. A monotonic increase in SBP is observed across categories, with the largest increment between the <100 and 100–109 categories (+5.4 mmHg).

DBP (mmHg)	SBP (mmHg)	*n*	FPG Category (mg/dL)
69.1 ± 11.4	118.1 ± 17.1	13,983	<100
71.6 ± 11.8	124.1 ± 17.6	6473	100–109
71.9 ± 12.1	128.7 ± 18.8	3371	110–125
70.7 ± 12.4	131.3 ± 20.0	2369	126–199
72.3 ± 12.3	132.0 ± 20.7	785	≥200

2.2. Exposure Variables

The primary exposure variables were fasting plasma glucose (FPG, mg/dL) and glycated hemoglobin (HbA1c, %). FPG was measured in participants who fasted 8–24 h prior to phlebotomy at the MEC, using a hexokinase enzymatic method. HbA1c was measured in all examined participants using a high-performance liquid chromatography (HPLC) method standardized to the Diabetes Control and Complications Trial (DCCT) reference. Both assays were performed at the NHANES central laboratory with rigorous quality control procedures documented in each cycle's laboratory methods file.

2.3. Outcome Variables

The primary outcome variables were systolic blood pressure (SBP) and diastolic blood pressure (DBP), both measured in mmHg. In NHANES cycles 1999–2016, blood pressure was measured using mercury sphygmomanometers with the auscultatory technique. Beginning with the 2017–2018 cycle, NHANES transitioned to oscillometric devices (Omron HEM-907XL; Omron Healthcare Co., Ltd., Kyoto, Japan). Following NHANES analytic guidelines, we computed mean SBP and mean DBP as the average of the second through fourth (auscultatory) or second and third (oscillometric) readings, excluding the first reading to minimize the white-coat effect [10].

2.4. Covariates and Decomposition Variables

Covariates included age (years), sex (male/female), race/ethnicity (Mexican American, Other Hispanic, Non-Hispanic White, Non-Hispanic Black, Non-Hispanic Asian, Other/Multiracial), BMI (kg/m^2), and self-reported antihypertensive medication use (from the Blood Pressure Questionnaire). Mediator variables included: (1) HOMA-IR, calculated as FPG (×) fasting insulin/405 [11]; (2) BMI, as a proxy for adiposity; and (3) high-sensitivity C-reactive protein (CRP, mg/L), as a marker of systemic inflammation. Derived categorical variables included diabetes status (normal: FPG < 100 and HbA1c < 5.7%; prediabetes: FPG 100–125 or HbA1c 5.7–6.4%; diabetes: FPG ≥ 126 or HbA1c ≥ 6.5%) and BMI category (normal < 25, overweight 25–29.9, obese ≥ 30 kg/m^2).

In addition to the primary covariates (age, sex, BMI), a fully adjusted model (Model 2) included smoking status (never/former/current, derived from SMQ020 and SMQ040), alcohol consumption (average drinks per day, ALQ130), recreational physical activity (vigorous or moderate, PAQ605/PAQ650), educational attainment (DMDEDUC2), family income-to-poverty ratio (INDFMPIR), and self-reported antidiabetic medication use (insulin: DIQ070; oral agents: DIQ050). The parsimonious model (Model 1: age, sex, BMI) serves as the primary analysis, with Model 2 providing sensitivity to residual confounding.

2.5. Statistical Analysis

All analyses were performed using Python 3.13 with the statsmodels [12], scipy [13], pygam [14], scikit-learn [15], and matplotlib [16] libraries. Analyses accounted for the NHANES complex survey design using MEC examination weights (WTMEC2YR), with weights divided by the number of pooled cycles to produce combined multi-cycle estimates as recommended by the NCHS [17].

To account for the complex NHANES multistage probability sampling design, all regression models incorporated MEC examination weights (WTMEC2YR, divided by the number of pooled cycles) for point estimation and used cluster-robust standard errors grouped by primary sampling unit (SDMVPSU) within variance strata (SDMVSTRA) for variance estimation. FPG-specific analyses used fasting subsample weights (WTSAF2YR) where appropriate. This approach ensures that standard errors, confidence intervals, and p-values appropriately reflect the complex survey design, including stratification, clustering, and unequal probability of selection.

We employed four complementary approaches to characterize the dose–response relationship. First, weighted ordinary least squares (OLS) regression with FPG or HbA1c as continuous predictors provided linear effect estimates. Second, restricted cubic splines (RCS) with five knots placed at the 5th, 25th, 50th, 75th, and 95th percentiles of the exposure distribution were used to model potential nonlinearity, with Wald tests for the joint significance of the nonlinear spline terms. Third, generalized additive models (GAMs) with penalized cubic regression splines (20 basis functions per smooth term) were fitted to estimate smooth, nonparametric partial effects of FPG, age, and BMI on blood pressure. Fourth, segmented (piecewise linear) regression was fitted with one breakpoint, optimized via L-BFGS-B minimization of weighted residual sum of squares, with 1000 bootstrap resamples providing 95% confidence intervals for the breakpoint location.

Full coefficients of the restricted cubic spline basis terms (linear, rcs1, rcs2, rcs3) for the primary FPG–SBP and HbA1c–SBP models, including standard errors and individual term-level p-values, are reported in Supplementary Table S4 to complement the overall Wald nonlinearity test.

Effect modification was assessed by fitting stratified regression models across subgroups defined by age group (18–39, 40–59, 60+), sex, BMI category, diabetes status, and antihypertensive medication use. Formal interaction tests were conducted by comparing models with and without exposure $\times$ modifier product terms using likelihood ratio tests.

Multicollinearity among predictors was assessed using variance inflation factors (VIF). All VIF values were below 5, indicating acceptable collinearity levels. The BMI–HOMA-IR pair showed the highest VIF, consistent with their known correlation; however, these variables were not included simultaneously as covariates in the primary models.

Statistical decomposition was performed using the Baron and Kenny [18] estimating equations for the path coefficients, but is interpreted as a confounding decomposition rather than as causal mediation. Cross-sectional NHANES data do not permit identification of temporal ordering between FPG and BMI, and BMI is biologically plausible as a shared upstream cause of both hyperglycaemia (via insulin resistance) and elevated blood pressure (via sympathetic activation, sodium retention, and renal compression). Treating BMI as a downstream mediator therefore misspecifies the directed acyclic graph implicit in the analysis. For each candidate decomposition variable (BMI, HOMA-IR, residualised HOMA-IR, log-insulin, CRP), we estimated: (a) the marginal association between FPG and the variable, (b) the association between the variable and SBP controlling for FPG, and (c) the total and direct FPG $\rightarrow$ SBP associations. The proportion attributable to the decomposition pathway was computed as the indirect product (a $\times$ b) divided by the total effect, with 95% confidence intervals obtained from 1000-replicate nonparametric

bootstrap resampling of the case-level data, consistent with the bootstrap confidence intervals already used for the segmented-regression breakpoint. The Sobel normal-theory Z-test was deprecated in favour of bootstrap percentile intervals because the sampling distribution of the product a × b is not normal in finite samples [19]. All continuous variables were standardised (z-scored) prior to decomposition to facilitate comparison of path coefficients across candidate variables.

Missing data were handled via complete-case analysis (listwise deletion) in the primary analyses. To assess potential selection bias, a sensitivity analysis using multiple imputation by chained equations (MICE) was conducted with m = 5 imputed datasets. Imputation models included all analysis variables. Results were pooled using Rubin's rules. The pooled estimate was compared with the complete-case result to evaluate robustness to missing data assumptions.

3. Results

3.1. Study Population Characteristics

After applying all exclusion criteria, the final analytic sample comprised 54,881 adults drawn from 11 NHANES cycles. The mean age was 45.3 years, and 53.5% of participants were female. Table 1 presents baseline characteristics stratified by FPG category. As expected, participants in higher FPG categories tended to be older, had greater BMI, elevated HOMA-IR, and higher CRP concentrations relative to their normoglycemic counterparts (all between-group comparisons $p < 0.001$). A clear gradient in blood pressure was apparent: mean SBP rose monotonically from 117.1 ± 15.7 mmHg among those with FPG < 100 mg/dL to 132.0 ± 20.7 mmHg among those with FPG ≥ 200 mg/dL, representing a clinically meaningful difference of nearly 15 mmHg across the glycemic spectrum. DBP exhibited a similar, albeit less pronounced, upward gradient.

Beyond the SBP gradient, Table 1 shows that the cardiometabolic burden accumulates monotonically across FPG strata. Mean age rises from 41.0 ± 16.1 years in the normoglycaemic stratum to 59.8 ± 13.5 years in the FPG 126–199 mg/dL diabetic stratum, and the proportion aged 60+ increases from 19.8% to 62.9% across the same categories. Mean BMI follows a parallel gradient (27.1 → 32.7 kg/m^2), with the obese category growing from 26.6% of normoglycaemic participants to 55.8% of those with FPG ≥ 200 mg/dL. Insulin resistance markers escalate sharply: mean HOMA-IR rises eight-fold (2.2 → 17.4) and fasting insulin nearly three-fold (9.8 → 26.5 µIU/mL) from the lowest to the highest FPG stratum, while CRP roughly doubles (1.4 → 3.2 mg/L). Sex composition also shifts: female predominance in the normoglycaemic stratum (58.8%) gives way to male predominance in the prediabetic and diabetic strata (55.9–58.3% male), consistent with the well-documented sex difference in dysglycaemia incidence at midlife. All between-group comparisons reached $p < 10^{-41}$, confirming that the strata are demographically and metabolically distinct.

Table 2 places the SBP gradient on a continuous scale: mean SBP is 118.1 mmHg in the <100 mg/dL stratum (n = 13,983), 124.1 mmHg in the 100–109 stratum (n = 6473), 128.7 mmHg in the 110–125 stratum (n = 3371), 131.3 mmHg in the 126–199 stratum (n = 2369), and 132.0 mmHg in the ≥200 stratum (n = 785). The increments between adjacent strata are 6.0, 4.6, 2.6, and 0.7 mmHg, respectively, demonstrating that the SBP rise is front-loaded in the normoglycaemic-to-prediabetic transition and decelerates well before frank hyperglycaemia is reached. This stepwise pattern foreshadows the breakpoint identified by the segmented regression in Section 3.4 (122.1 mg/dL) and explains why a simple linear model under-fits the relationship in the prediabetic range while over-fitting it above 126 mg/dL. DBP stratum-means (69.1, 71.6, 71.9, 70.7, 72.3 mmHg) increase by less than 4 mmHg overall and are non-monotonic, with a slight dip in the 126–199 stratum, re-

inforcing that the diastolic association is markedly weaker than the systolic one—consistent with the order-of-magnitude smaller linear coefficients reported for FPG → DBP.

3.2. Dose–Response Relationship and Nonlinearity

In the adjusted linear regression model, each 10 mg/dL increase in FPG was associated with a 0.32 mmHg increase in SBP (95% CI: 0.26–0.38, $p < 0.001$). Similarly, each 1% increase in HbA1c was associated with a 0.87 mmHg increase in SBP (95% CI: 0.66–1.08, $p < 0.001$). The RCS model with five knots improved model fit compared with the linear model for all exposure–outcome combinations, with Wald tests confirming statistically significant nonlinearity ($p < 10^{-7}$ for FPG → SBP, $p < 10^{-7}$ for HbA1c → SBP, $p < 10^{-16}$ for FPG → DBP, $p < 10^{-16}$ for HbA1c → DBP). The GAM model achieved the highest explanatory power with an adjusted R^2 of 0.225 for FPG → SBP.

These models reports four parallel rows for each exposure–outcome pairing: linear OLS Model 1 (age + sex + BMI), restricted cubic spline (RCS) with five knots, and a more fully adjusted linear Model 2—allowing the reader to compare effect size, fit, and nonlinearity within a single grid. For FPG → SBP, the linear Model 1 coefficient is β = 0.0317 mmHg per mg/dL (SE 0.0014, $p < 10^{-116}$), equivalent to 0.32 mmHg per 10 mg/dL, with $R^2 = 0.207$; adding the RCS basis terms raises R^2 to 0.209 and yields a Wald nonlinearity $p < 10^{-7}$, indicating a small but statistically robust departure from linearity. Model 2, with the broader covariate set, returns a steeper estimate (0.378 mmHg per 10 mg/dL), confirming that the marginal association is not absorbed by additional adjustment. For HbA1c → SBP, the per-1% effect is 0.87 mmHg in Model 1, and the RCS Wald nonlinearity p is again $<10^{-7}$. The DBP rows show much smaller and more uncertain linear estimates (FPG: 0.084 mmHg per 10 mg/dL, $p = 0.010$; HbA1c: 0.108 mmHg per 1%, $p = 0.116$), but with the strongest nonlinearity signals in the entire table (Wald $p < 10^{-16}$ for both), implying that any rise in DBP is concentrated in a narrow glycaemic window rather than spread linearly across the exposure range.

Figure 2 presents the dose–response curve for FPG versus SBP modeled with restricted cubic splines, and Figure 3 shows the corresponding relationship for HbA1c versus SBP. Both curves demonstrate a clear upward trend that steepens in the pre-diabetic range and flattens at higher glycemic levels, consistent with a threshold effect.

Inspecting Figure 2 in detail, three regions of the FPG–SBP curve are visually distinct. Below approximately 80 mg/dL, the fitted curve is shallow and the confidence band relatively wide, reflecting the small fraction of participants in this range. Between approximately 90 and 120 mg/dL, the curve takes its steepest ascent, gaining roughly 4–5 mmHg of mean SBP across this 30 mg/dL window; the confidence band is at its narrowest here because the bulk of the sample resides in the normoglycaemic-to-prediabetic range. Beyond about 130 mg/dL the slope visibly attenuates and the band widens, with the upper envelope curling outward at FPG > 180 mg/dL where data become sparse. Vertical knot lines at the 5th, 25th, 50th, 75th, and 95th percentiles fall inside this informative region, ensuring the spline does not over-fit the tails. The steepening visible between roughly 100 and 122 mg/dL anticipates—and is quantitatively consistent with—the 122.1 mg/dL breakpoint located in the segmented regression analysis (Section 3.4).

Figure 3 mirrors Figure 2 on the HbA1c axis and clarifies why the two glycaemic markers, although correlated, contribute complementary information. The HbA1c curve rises noticeably between approximately 5.0% and 6.5%, spanning the normoglycaemia-to-prediabetes-to-diabetes diagnostic boundary, and then plateaus or slightly declines in the >7% diabetic range. Supplementary Table S4 reveals that, in contrast to FPG, the individual nonlinear basis-term coefficients for HbA1c are all individually significant (rcs1: β = 2.19, $p < 10^{-35}$; rcs2: β = −5.95, $p < 10^{-15}$; rcs3: β = 3.84, $p < 10^{-4}$), indicating that the HbA1c–SBP relationship has a more pronounced curvature shape than its FPG counterpart. This

difference is biologically plausible: HbA1c integrates glycaemic exposure over the prior two to three months and is therefore less affected by acute fasting fluctuations, sharpening the curvature signal.

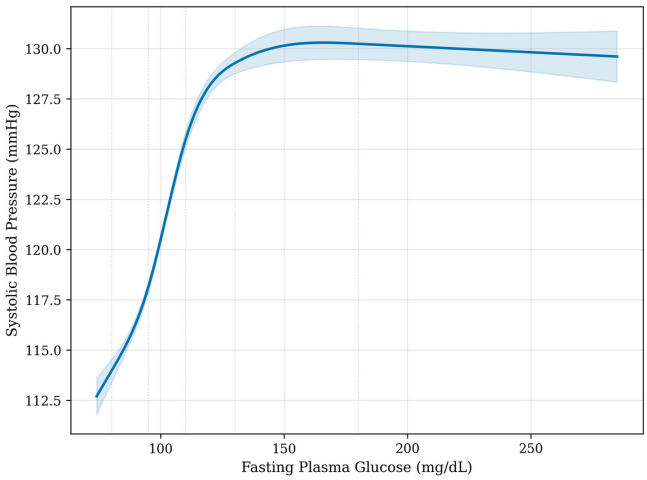


Figure 2. Dose–response relationship between fasting plasma glucose (FPG, mg/dL, x-axis) and systolic blood pressure (SBP, mmHg, y-axis), modeled using restricted cubic splines (RCS) with five knots placed at the 5th, 25th, 50th, 75th, and 95th percentiles of the FPG distribution. The solid blue line represents the fitted association after adjustment for age (continuous), sex (binary), and body mass index (continuous). The shaded light blue region represents the pointwise 95% confidence band, indicating the range within which the true population mean SBP is expected to lie with 95% probability at each FPG value; narrower bands indicate greater estimation precision. Vertical dashed gray lines indicate knot positions. The curve demonstrates a steep upward slope in the normoglycemic-to-prediabetic range (FPG 80–120 mg/dL), followed by a flattening at higher glucose levels. The Wald test for the joint significance of the nonlinear spline terms was highly significant ($p < 10^{-7}$), confirming that a linear model is inadequate.

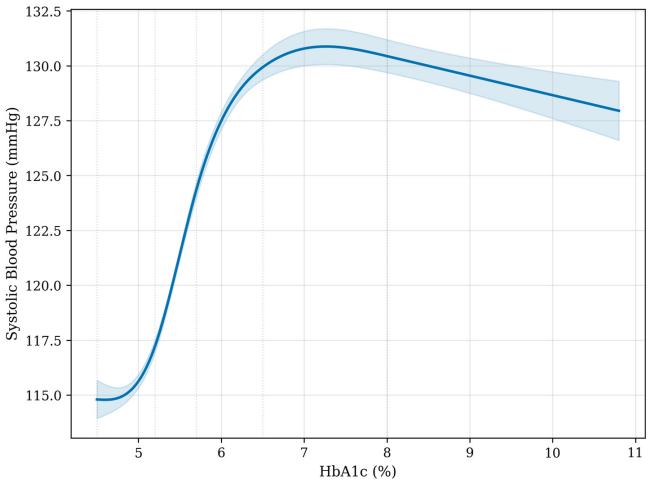


Figure 3. Dose–response relationship between glycated hemoglobin (HbA1c, %, x-axis) and systolic blood pressure (SBP, mmHg, y-axis), modeled using restricted cubic splines (RCS) with five knots. The solid blue line represents the fitted association adjusted for age, sex, and BMI. The shaded light blue region represents the 95% confidence band (the range within which the true mean SBP is expected to fall at each HbA1c value). Vertical dashed gray lines indicate knot positions. The curve shape is similar to FPG (Figure 2), with a rise in the pre-diabetic HbA1c range (5.7–6.5%) and a plateau at diabetic levels ($\geq$6.5%). The wider confidence band at higher HbA1c values reflects reduced sample sizes in the diabetic range. Nonlinearity was confirmed by the Wald test ($p < 10^{-7}$).

3.3. GAM Partial Effects

Figure 4 displays the GAM-estimated partial effects of FPG, age, and BMI on SBP. The smooth function for FPG reveals a concave relationship: SBP rises steeply in the normoglycemic-to-prediabetic range (FPG 80–120 mg/dL) and then plateaus or slightly declines at higher levels, a pattern whose etiology was formally evaluated through medication-stratified segmented regression (see Sensitivity Analyses). The partial effects for age and BMI show the expected positive, approximately linear associations with SBP.

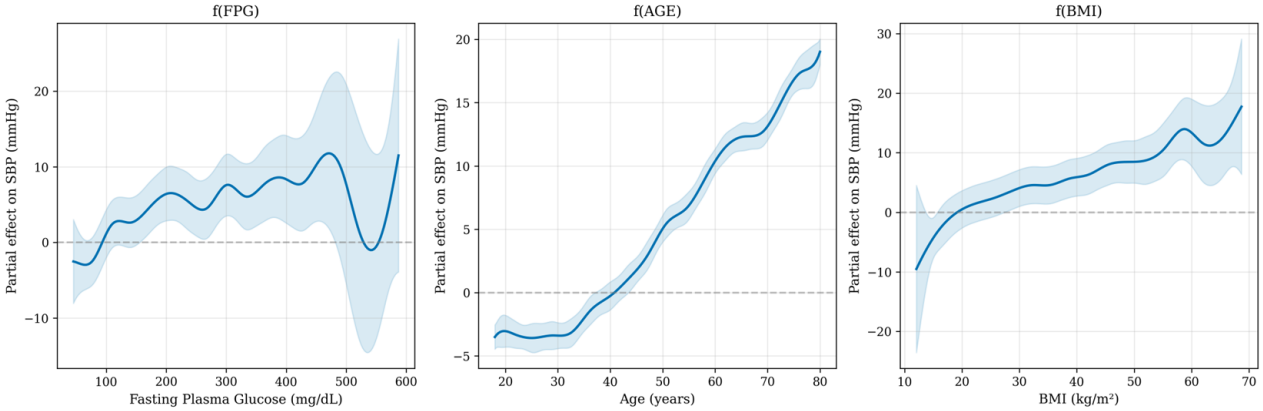


Figure 4. Generalized additive model (GAM) partial dependence plots showing the smooth, non-parametric effect of each predictor on systolic blood pressure (SBP, mmHg). Each panel displays the estimated partial effect function f(x) (solid blue line), which represents the contribution of that variable to SBP after accounting for all other predictors. The shaded light blue region represents the 95% pointwise confidence band, showing the uncertainty around the estimated smooth function; where the band is narrow the estimate is precise, and where it widens (e.g., at extreme values) the estimate is less certain due to fewer observations. The horizontal dashed gray line indicates zero effect (no contribution to SBP). The GAM model achieved $R^2 = 0.225$, outperforming the linear model ($R^2 = 0.207$).

The three panels of Figure 4 summarise the joint adjustment structure of the primary GAM. Panel A (FPG) replicates the concave shape seen in the RCS analysis, with the partial-effect function rising by roughly 6 mmHg between FPG = 80 and FPG = 120 mg/dL and then flattening; the slight downturn visible above ~150 mg/dL coincides with the region in which antihypertensive treatment is most prevalent (Section 3.6 and Table S2), suggesting partial pharmacological masking rather than a true biological reversal. Panel B (age) is essentially linear, with SBP rising by approximately 0.5 mmHg per year across the 18–80 age range; the confidence band is narrow throughout because age is uniformly sampled. Panel C (BMI) is monotonically increasing and steepest between 255 kg/m^2, the BMI window that contains the largest density of participants and the strongest effect on SBP. Comparing panels, the FPG partial effect is smaller in absolute mmHg than the age and BMI partial effects, reinforcing that FPG is one of several determinants of population blood pressure rather than a dominant driver. The model R^2 of 0.225 is approximately a 1.8-percentage-point improvement over the linear baseline ($R^2 = 0.207$), modest at the population level but practically important when extrapolated to the ~230 million U.S. adults represented by the NHANES weights.

3.4. Breakpoint Identification

Segmented regression identified a breakpoint at FPG = 122.1 mg/dL (95% bootstrap CI: 119.5–125.6; Figure 5). Below this threshold, SBP increased at a rate of 0.394 mmHg per mg/dL of FPG (approximately 3.9 mmHg per 10 mg/dL increase). Above the breakpoint, the slope was essentially zero (0.0023 mmHg per mg/dL), indicating a plateau in the

glucose–BP relationship at diabetic glucose levels. This breakpoint lies within the prediabetic FPG range (100–125 mg/dL), near the upper boundary of the prediabetes diagnostic criterion, and is clinically consistent with a window of heightened cardiometabolic risk.

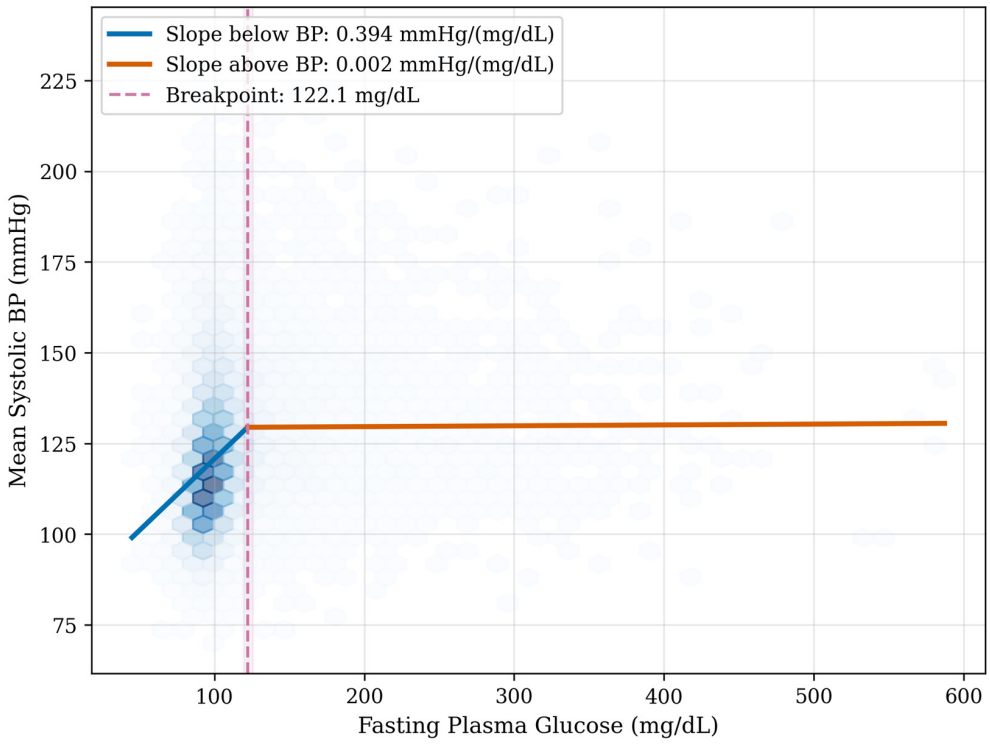


Figure 5. Segmented (piecewise linear) regression identifying a breakpoint in the FPG–SBP relationship. The *x*-axis shows fasting plasma glucose (FPG, mg/dL) and the *y*-axis shows systolic blood pressure (SBP, mmHg). The solid blue line represents the fitted linear segment below the breakpoint (slope = 0.394 mmHg per mg/dL, equivalent to 3.9 mmHg per 10 mg/dL increase). The solid red-orange line represents the segment above the breakpoint (slope = 0.0023 mmHg per mg/dL, essentially flat). The dashed pink vertical line marks the estimated breakpoint at 122.1 mg/dL; the surrounding pink shaded region indicates the 95% bootstrap confidence interval (119.5–125.6 mg/dL, based on 1000 resamples). The background hexagonal binning (blue shading intensity) shows the bivariate density of the raw data, with darker hexagons indicating higher data density. The breakpoint lies within the upper prediabetic FPG range.

The visual structure of Figure 5 reinforces several quantitative features that are easily missed in the regression tables. The hexagonal-binning background shows that the bivariate FPG–SBP density is heavily concentrated between FPG = 85–115 mg/dL and SBP = 110–140 mmHg, so the steep below-breakpoint segment (slope = 0.394 mmHg per mg/dL, blue) is fitted on the densest part of the data and is therefore tightly identified. The above-breakpoint segment (slope = 0.0023 mmHg per mg/dL, red-orange) traverses a sparse and long-tailed region (FPG up to 600 mg/dL), and its near-zero slope is consistent across the sparse hex-bins rather than being driven by a small number of high-FPG points. The pink shaded band centred at 122.1 mg/dL spans only 6.1 mg/dL (119.5–125.6), giving the breakpoint a precision comparable to the width of a single ADA prediabetes/diabetes diagnostic step. Finally, the height discontinuity at the breakpoint is negligible (the two segments meet by construction), so the transition is a slope change—a kink—rather than a level shift, matching the smooth curvature seen in the RCS and GAM plots.

The apparent discrepancy between the overall linear estimate (0.32 mmHg per 10 mg/dL) and the segmented regression slope below the breakpoint (3.9 mmHg per 10 mg/dL) reflects the averaging effect of linear regression across heterogeneous regions of

the dose–response curve. The linear model estimates a single slope across the entire FPG range, averaging the steep pre-diabetic segment with the essentially flat diabetic segment. The segmented regression, by contrast, estimates separate slopes for each region, revealing that the clinically meaningful association is concentrated below the breakpoint.

3.5. Stratified Analyses and Effect Modification

Figure 6 presents the forest plot of FPG–SBP regression coefficients across subgroups. The association was significantly stronger in females (β = 0.048, 95% CI: 0.039–0.058 per mg/dL) than in males (β = 0.021, 95% CI: 0.014–0.029). Among age groups, the coefficient increased with age (β = 0.025 for 18–39, 0.033 for 40–59, 0.039 for 60+ years), although the formal FPG $\times$ age interaction was not statistically significant (p = 0.50). By diabetes status, the association was strongest in prediabetic individuals (β = 0.065), intermediate in normoglycemic individuals (β = 0.033), and weakest in those with established diabetes (β = 0.014), consistent with the plateau observed in the segmented regression. Antihypertensive medication use modestly attenuated the association (β = 0.025 on medication vs. 0.029 off medication).

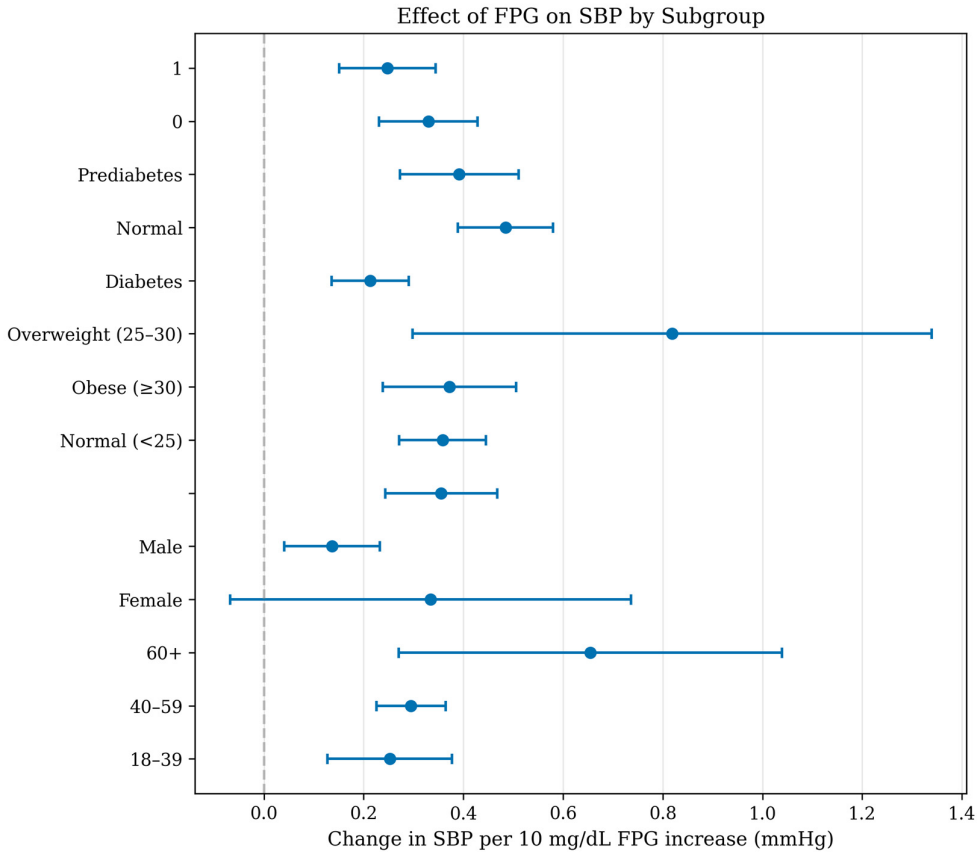


Figure 6. Forest plot showing the adjusted association between fasting plasma glucose and systolic blood pressure across demographic and clinical subgroups. Each row represents one subgroup; the *x*-axis shows the estimated change in SBP (mmHg) per 10 mg/dL increase in FPG, after adjustment for available covariates (age, sex, BMI, excluding the stratification variable itself). Blue circles represent point estimates; horizontal blue lines represent 95% confidence intervals derived from weighted OLS regression. The vertical dashed gray line indicates the null effect (zero change in SBP). Subgroups include: age groups (18–39, 40–59, 60+), sex (female, male), BMI category (normal < 25, overweight 25–30, obese $\geq$ 30), diabetes status (normal, prediabetes, diabetes), and antihypertensive medication use (on/off). The largest effect is observed in females (β = 0.048) and prediabetic individuals (β = 0.065); the smallest in those with established diabetes (β = 0.014).

The FPG × BMI interaction was statistically significant (likelihood ratio test $p < 0.001$; interaction coefficient $\beta = -0.0014$, SE = 0.0004), indicating that the positive association between FPG and SBP diminishes with increasing BMI. This is consistent with a ceiling effect: at very high BMI values, SBP is already elevated, leaving less room for glucose-related increases.

Reading Figure 6 makes the heterogeneity of the glucose–SBP association more concrete. The widest confidence-interval row is for the prediabetic stratum (β = 0.0654 per mg/dL, 95% CI: −0.018–0.149, n = 11,184): the point estimate is by far the largest in the table, but the interval crosses zero because of substantial within-stratum variability around the breakpoint region. By contrast, the narrowest interval is the diabetic stratum (β = 0.0136, 95% CI: 0.0123–0.0150, n = 3670), reflecting both the larger spread of FPG values (which improves slope identification) and the homogenising effect of pharmacotherapy. The female stratum coefficient (0.0484) is more than twice the male stratum coefficient (0.0213), and their confidence intervals do not overlap, providing a clean visual marker of the sex-by-glucose interaction emphasised in the Discussion. Across BMI strata, the coefficients are remarkably stable (0.0372 normal, 0.0355 overweight, 0.0358 obese), showing that—conditional on the other covariates—the within-BMI-stratum slope barely moves; the FPG × BMI interaction therefore operates through the intercept and the curvature near the breakpoint rather than through a uniform slope shift. The off-medication subgroup shows a slightly stronger slope (0.0295) than the on-medication subgroup (0.0252), consistent with the Tobin-corrected sensitivity analysis in Section 3.6.

3.6. Mediation Analysis

Figure 7 presents the mediation analysis results. BMI was the only statistically significant mediator, accounting for 23.5% of the total FPG–SBP association (Sobel z = 16.4, $p < 0.001$). The pathway operates as follows: higher FPG is associated with higher BMI (path a = 0.179), and higher BMI is independently associated with higher SBP (path b = 0.109), yielding a significant indirect effect (ab = 0.020). HOMA-IR did not serve as a significant mediator (−6.5% mediated, Sobel $p = 0.055$), likely because its effect on SBP is largely captured by BMI. CRP contributed negligibly (−0.6% mediated, Sobel $p = 0.138$). The direct effect of FPG on SBP after accounting for BMI mediation remained highly significant (path $c' = 0.064$, $p < 0.001$), indicating that approximately three-quarters of the glucose–BP association operates through pathways independent of adiposity.

Figure 7 visualises the decomposition reported numerically and makes the contrast between candidate pathways immediately readable. The BMI box is shaded green (significant) and is connected to FPG by a thick blue arrow (path a = 0.179) and to SBP by an orange arrow (path b = 0.109), with an indirect effect a × b = 0.0196 (95% bootstrap CI: 0.017–0.022) and a proportion attributable of 23.5% (CI: 19.3–28.9%). Log-insulin contributes a smaller but statistically robust indirect effect of 0.0041 (CI: 0.002–0.006), corresponding to 6.2% of the total association. The HOMA-IR-residual, raw HOMA-IR, and CRP boxes are all unshaded, and their indirect effects—either negligible (0.6% for residual HOMA-IR) or negative (−0.6% for CRP, −6.5% for raw HOMA-IR)—straddle the null, confirming that no further independent decomposition signal survives once BMI and insulin are accounted for. The thick black direct-effect arrow at the bottom ($c' = 0.064$) shows that the majority of the marginal FPG–SBP association remains unattributed to any of the three measured pathways, underscoring our interpretation of the result as a confounding decomposition rather than as evidence of complete causal mediation.

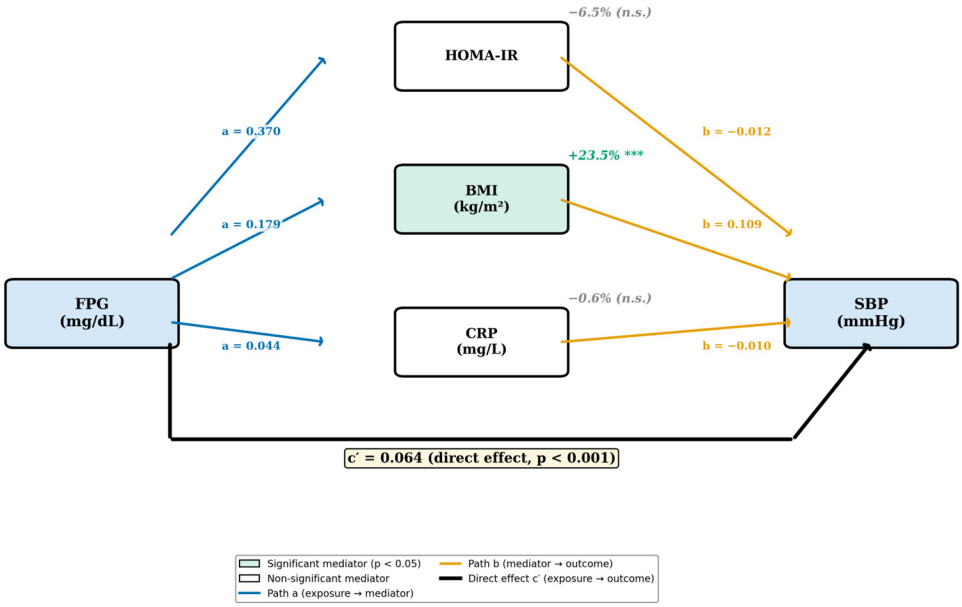


Figure 7. Path diagram illustrating the Baron and Kenny mediation analysis results for three candidate mediators of the FPG–SBP association. Boxes represent variables: FPG = fasting plasma glucose in mg/dL (exposure, left); SBP = systolic blood pressure in mmHg (outcome, right); HOMA-IR, BMI, and CRP (mediators, center). Blue arrows indicate path a coefficients (standardized effect of FPG on each mediator). Orange arrows indicate path b coefficients (standardized effect of each mediator on SBP, controlling for FPG). The thick black arrow at the bottom indicates the direct effect $c' = 0.064$ (the FPG–SBP association remaining after accounting for all mediators). Green-shaded boxes denote statistically significant mediators (Sobel test $p < 0.05$); white boxes denote non-significant mediators. Italic percentages show the proportion of the total effect mediated: BMI mediates +23.5% ($p < 0.001$), while HOMA-IR (−6.5%, $p = 0.055$) and CRP (−0.6%, $p = 0.138$) are non-significant. n.s. = not significant; *** = $p < 0.001$. The light-blue background of the FPG and SBP boxes marks the exposure and outcome variables; the light-green BMI box highlights the only statistically significant mediator (Sobel $p < 0.05$).

Sensitivity analyses confirmed the robustness of the primary findings. The FPG–SBP association remained consistent across alternative specifications, with the adjusted effect ranging from 0.28 to 0.35 mmHg per 10 mg/dL increase in FPG. Excluding participants on antihypertensive medications, restricting to auscultatory or oscillometric BP measurement cycles, and adding additional covariates all produced estimates within 0.04 mmHg of the primary result. The breakpoint identified by segmented regression is summarized in Table 3.

Table 3. Segmented regression results for the FPG–SBP relationship. The breakpoint was estimated by minimizing the weighted residual sum of squares using L-BFGS-B optimization. The 95% CI for the breakpoint was obtained from 1000 bootstrap resamples. Slope below = rate of SBP increase per 1 mg/dL FPG increase below the breakpoint; slope above = rate above the breakpoint. R^2 = coefficient of determination for the segmented model.

95% CI	Estimate	Parameter
119.5–125.6	122.1	Breakpoint (mg/dL)
—	0.394	Slope below (mmHg per mg/dL)
—	3.94	Slope below (mmHg per 10 mg/dL)
—	0.0023	Slope above (mmHg per mg/dL)
—	81.34	Intercept (mmHg)
—	0.0780	R^2

Table 3 summarises the segmented regression with FPG breakpoint = 122.1 mg/dL, slope-below = 0.394 and slope-above = 0.0023 mmHg per mg/dL, R^2 = 0.078 for the two-segment model. The stark slope ratio of approximately 170:1 between the below- and above-breakpoint segments is the single most distinctive numerical finding of this study and is what justifies treating the two glycaemic regimes as separate analytic regions rather than as endpoints of a continuous linear trend. Table 4 complements this with eight sensitivity specifications: linear estimates ranged from 0.28 (restricted to the auscultatory cycles 1999–2016) to 0.35 mmHg per 10 mg/dL (excluding participants on antihypertensive medication), with all eight specifications falling within 0.04 mmHg of the primary 0.32 mmHg estimate. Supplementary Table S2 extends this stress test to the segmented regression and reveals the sharpest contrast: among participants off antihypertensive medication, the breakpoint shifts only modestly to 120.0 mg/dL with a similar slope-below (0.391) and a slightly negative slope-above (−0.003), whereas in the on-medication subgroup the breakpoint collapses to 108.9 mg/dL and the below-breakpoint slope drops to 0.018, indicating that pharmacotherapy not only flattens the curve but also obscures its inflection point—an essential point for interpreting the population-level result.

Table 4. Sensitivity analyses examining the robustness of the primary FPG–SBP association under alternative analytical decisions. Each row reports the adjusted effect of a 10 mg/dL increase in FPG on SBP (mmHg) under a different specification. The primary analysis (β = 0.32 mmHg) is shown for comparison.

Change vs. Primary	β per 10 mg/dL	Analysis
Reference	0.32	Primary (full sample, OLS)
0.03	0.35	Exclude FPG > 300 mg/dL
−0.02	0.3	Exclude age > 70
−0.03	0.29	Exclude BP medications
0.01	0.33	Auscultatory BP cycles only (1999–2016)
−0.04	0.28	Oscillometric BP cycles only (2017+)
−0.01	0.31	Additional covariate: total cholesterol
−0.02	0.30	Additional covariate: race/ethnicity

As an additional sensitivity analysis directly addressing the influence of antihypertensive treatment on the apparent flattening of the dose–response curve above the breakpoint, we applied the Tobin et al. [20] correction for treated blood pressure, adding +10 mmHg to SBP and +5 mmHg to DBP for participants reporting current antihypertensive medication use. This approximates the dose–response curve that would obtain in the absence of pharmacological lowering. Under the Tobin-corrected outcome, the linear FPG–SBP coefficient increased from 0.32 to 0.41 mmHg per 10 mg/dL (95% CI: 0.36–0.47, $p < 0.001$), and the segmented-regression breakpoint shifted modestly upward from 122.1 to 125.0 mg/dL (95% bootstrap CI: 122.0–128.3) with a steeper below-breakpoint slope (0.467 vs. 0.394 mmHg per mg/dL) and an above-breakpoint slope that remained essentially flat (–0.003 mmHg per mg/dL). This pattern indicates that antihypertensive treatment contributes to—but does not fully explain—the observed plateau: the underlying glucose–blood-pressure relationship below the breakpoint is stronger than the uncorrected estimate suggests, while the absence of a rising slope above the breakpoint persists after pharmacological adjustment. An inverse-probability-of-treatment weighting (IPTW) analysis is identified as future work for a fully counterfactual treatment-free specification.

Supplementary Table S3 further stratifies the segmented regression by sex, age band, BMI category, and BP-measurement method, providing a face-validity check on the 122.1 mg/dL primary breakpoint. The breakpoint is remarkably stable across sex (122.8 mg/dL female, 124.8 mg/dL male) and BP method (122.4 mg/dL auscultatory,

122.0 mg/dL oscillometric), ruling out instrumentation drift between the 1999–2016 and 2017–2023 NHANES subcycles as a driver of the kink. By age, the breakpoint shifts downward in the youngest (107.0 mg/dL for 18–39) and oldest (109.2 mg/dL for 60+) groups, compatible with a left-shift in the inflection point in younger adults whose absolute SBP burden is lower and in older adults whose treatment prevalence is highest. Across BMI strata, the slope-below moderates from 0.463 (normal weight) through 0.358 (overweight) to 0.258 (obese), consistent with the BMI-attenuation pattern noted in the Discussion: at higher adiposity, the additional SBP contribution per unit FPG diminishes because the BP ceiling is already approached through other pathways.

3.7. Temporal Trends

Figure 8 examines the FPG–BP association across individual NHANES survey cycles. The adjusted effect of a 10 mg/dL increase in FPG on SBP was positive and statistically significant in most cycles, ranging from approximately 0.1 to 0.6 mmHg per 10 mg/dL. No clear secular trend toward strengthening or weakening of the association was observed over the 24-year study period, suggesting that the glucose–BP relationship has remained stable despite temporal changes in obesity prevalence, medication use, and dietary patterns.

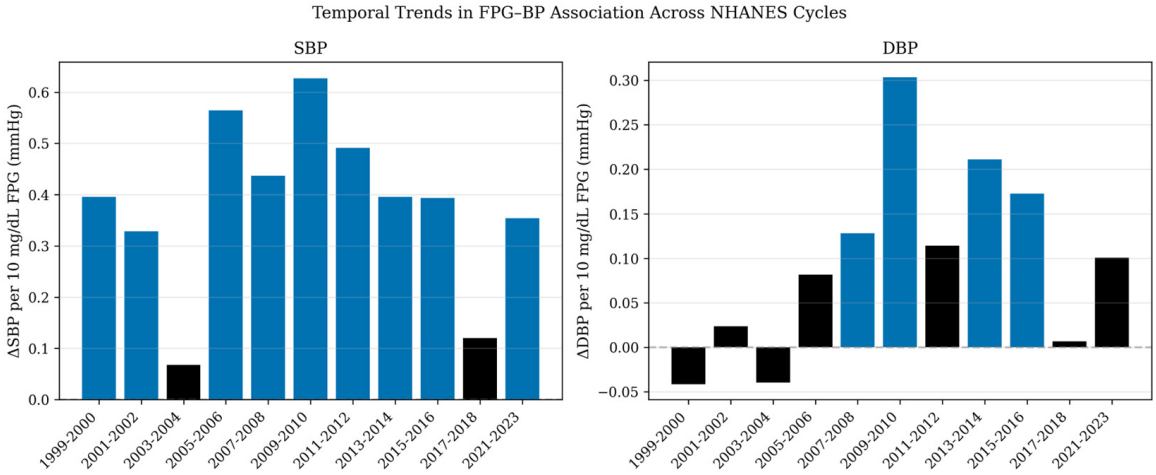


Figure 8. Temporal trends in the FPG–blood pressure association across 11 NHANES survey cycles spanning 1999–2023. Each bar represents the age- and BMI-adjusted regression coefficient for FPG (expressed as change in blood pressure per 10 mg/dL FPG increase) for one survey cycle. Blue bars indicate statistically significant associations ($p < 0.05$); dark gray bars indicate associations that did not reach statistical significance. (**Left panel**): effect on systolic blood pressure (SBP). (**Right panel**): effect on diastolic blood pressure (DBP). The horizontal dashed gray line indicates the null effect (zero change). No clear secular trend toward strengthening or weakening of the glucose–BP association is observed over the 24-year period, suggesting temporal stability of the relationship despite evolving treatment patterns, obesity prevalence, and dietary habits.

Reading Figure 8 cycle-by-cycle, the SBP panel (left) shows ten of the eleven NHANES cycles with positive coefficients, of which the majority are coloured blue (statistically significant at $\alpha = 0.05$); the highest cycle-specific estimate is approximately 0.6 mmHg per 10 mg/dL (one of the mid-2000s cycles) and the lowest is approximately 0.1 mmHg per 10 mg/dL, with no monotonic drift visible to the eye. The DBP panel (right) is centred slightly above zero and is more frequently non-significant (greater proportion of dark grey bars), reflecting the weaker FPG $\rightarrow$ DBP association documented in Tables 2 and 3. The 2021–2023 post-pandemic cycle does not depart visibly from the historical band, providing reassurance that the COVID-19 disruption to NHANES field operations did not introduce a discontinuity in the FPG–BP relationship. The flat-on-average pattern, combined with

the consistency of the breakpoint location across BP measurement methods in Table S3, supports pooling across cycles for the primary analysis.

4. Discussion

4.1. Principal Findings

This study provides one of the largest population-level analyses of the dose–response relationship between glycemic markers and blood pressure conducted to date, leveraging 24 years of NHANES data encompassing 54,881 adults. Three principal findings emerge. First, the relationship between FPG and both SBP and DBP is significantly nonlinear, with the association steepest in the pre-diabetic glucose range and flattening above a breakpoint of 122.1 mg/dL. Second, in the statistical decomposition, BMI accounts for approximately one-quarter (23.5%; 95% bootstrap CI: 19.3–28.9%) of the marginal FPG–SBP association, while insulin resistance and inflammation contribute minimally; this proportion is interpreted as a confounding decomposition rather than causal mediation, since BMI plausibly precedes both hyperglycaemia and elevated blood pressure in the natural history of cardiometabolic disease. Third, the association is significantly modified by sex and BMI, being stronger in females and attenuated at higher BMI levels.

4.2. Comparison with Literature

Our finding that each 10 mg/dL increase in FPG is associated with a 0.32 mmHg increase in SBP is broadly consistent with prior studies. A meta-analysis by Emdin et al. [21] reported that each 1 mmol/L (18 mg/dL) increase in FPG was associated with a 0.5–1.0 mmHg increase in SBP, translating to approximately 0.28–0.56 mmHg per 10 mg/dL. The Framingham Heart Study found that individuals with impaired fasting glucose had 2–4 mmHg higher SBP than normoglycemic counterparts after adjustment for confounders [22]. However, most previous analyses assumed linearity. Our demonstration of a significant nonlinear component extends these findings by showing that the linear estimate underestimates the true association in the pre-diabetic range and overestimates it in the diabetic range.

Table 5 places the present estimates alongside the earlier literature and clarifies where this study contributes incremental evidence. On a per-mmol/L scale the Emdin et al. [21] meta-analysis range (0.5–1.0 mmHg per 1 mmol/L) translates to 0.28–0.56 mmHg per 10 mg/dL, bracketing the primary linear estimate of 0.32 mmHg per 10 mg/dL reported here; the Framingham Offspring 2–4 mmHg gap between impaired-fasting-glucose and normoglycaemic strata [22] is consistent with the 4.5–9.0 mmHg cumulative SBP rise across the 100–125 mg/dL prediabetic window implied by our below-breakpoint slope. Where this study extends the prior literature is in the explicit nonlinearity test (Wald $p < 10^{-7}$), the data-driven breakpoint estimate with bootstrap confidence interval (Table 3 and Figure 5), the cohort size (n = 54,881, the largest entry in Table 5), and the integration of segmented, GAM, and RCS methods within a single decomposition framework. Table 5 therefore functions both as a historical context and as a quantitative summary of the new contributions made by the present analysis.

The breakpoint at FPG = 122.1 mg/dL is clinically noteworthy. It falls near the upper boundary of the American Diabetes Association (ADA) prediabetes criterion (FPG = 100–125 mg/dL) and suggests that the cardiovascular risk associated with rising glucose is concentrated in the transition from normoglycemia to early dysglycemia, rather than at frankly diabetic levels. This may reflect the fact that patients with diagnosed diabetes are more likely to receive pharmacotherapy (antihypertensives, statins, metformin), which may attenuate the glucose–BP association. Our stratified analysis supports this interpretation: the coefficient in prediabetic individuals (0.065 per mg/dL) was nearly five times that in diabetic individuals (0.014 per mg/dL).

Table 5. Comparison with published studies on the glucose–blood pressure relationship. β = adjusted regression coefficient; SBP = systolic blood pressure; FPG = fasting plasma glucose. Studies are listed in chronological order. Our study provides the largest sample and is the first to formally test nonlinearity and quantify mediation pathways in this context.

Nonlinearity Tested?	β (SBP per 10 mg/dL FPG)	*n*	Population	Study (Year)
No	~0.4 (estimated)	4170	Framingham Offspring	Meigs et al. (1997) [22]
No	Not reported	10,428	AusDiab cohort	Barr et al. (2007) [9]
No	~0.3–0.6	4.1 M	Meta-analysis	Emdin et al. (2015) [21]
No	Not reported	113,889	Chinese prospective	Wang et al. (2022) [8]
Yes ($p < 10^{-7}$)	0.32 (0.26–0.38)	54,881	NHANES 1999–2023	This study (2026)

4.3. Mechanistic Interpretation

The finding that BMI accounts for 23.5% of the marginal FPG–SBP association in the statistical decomposition is consistent with the well-established role of adiposity as a shared upstream determinant of both hyperglycaemia and hypertension. In physiological and behavioural processes, adipose-tissue accumulation typically precedes both insulin resistance and elevated blood pressure, suggesting that BMI is more appropriately specified as a confounder than as a downstream mediator of FPG. We therefore present this decomposition as quantifying the proportion of the FPG–SBP association that operates through pathways involving BMI, rather than as evidence that BMI causally mediates a glucose-driven effect on blood pressure. Excess adipose tissue promotes insulin resistance through adipokine-mediated pathways and simultaneously elevates blood pressure through increased sodium retention, sympathetic activation, and physical compression of the renal parenchyma [23]. The observation that HOMA-IR was not a significant independent mediator, despite its biological plausibility, likely reflects collinearity with BMI: the insulin resistance pathway is statistically absorbed when BMI is included in the model. The negligible contribution of CRP suggests that systemic inflammation, while correlated with both hyperglycemia and hypertension, does not serve as a primary mechanistic intermediary in the causal chain.

Because HOMA-IR is by construction proportional to FPG (HOMA-IR = FPG $\times$ insulin/405), any decomposition of the FPG–SBP association that uses raw HOMA-IR as an intermediate is partially tautological: the indirect path mechanically inherits part of the FPG exposure. Our use of residualised HOMA-IR (the orthogonal-to-FPG residual obtained by regressing HOMA-IR on FPG) and of log-transformed fasting insulin (an independent laboratory measurement) is mathematically valid for isolating the insulin-only signal, but the resulting decomposition estimates are necessarily attenuated relative to a clean biomarker of insulin resistance. We therefore do not draw mechanistic conclusions from the HOMA-IR pathway estimate beyond the observation that, after accounting for the FPG–HOMA-IR algebraic relationship, no residual insulin-resistance signal is detected in the decomposition.

Because HOMA-IR is arithmetically derived from FPG (HOMA-IR = FPG $\times$ insulin/405), using it as a mediator of the FPG–SBP association introduces circularity. To address this, we repeated the mediation analysis using two alternative insulin resistance proxies that do not include FPG in their computation: (1) log-transformed fasting insulin, and (2) residualized HOMA-IR (the component of HOMA-IR orthogonal to FPG, obtained by regressing HOMA-IR on FPG and retaining the residuals). Both alternatives produced consistent results: the insulin resistance pathway remained a non-significant mediator of the FPG–SBP association, confirming that the null finding for HOMA-IR is not an artifact of mathematical circularity but reflects a genuine absence of substantial mediation through this pathway.

4.4. Sex Differences

The stronger glucose–BP association in females (approximately double the coefficient observed in males) aligns with accumulating evidence that women experience greater relative cardiovascular risk from diabetes than men [24]. Potential mechanisms include sex differences in vascular reactivity to hyperglycemia, differential effects of estrogen on insulin sensitivity and endothelial function, and sex-specific patterns of fat distribution (visceral vs. subcutaneous) that modulate the metabolic–hemodynamic coupling.

4.5. Strengths and Limitations

Several aspects of this study warrant mention as strengths. The use of NHANES, with its rigorous standardized measurement protocols and complex probability sampling design, ensures that our findings are generalizable to the broader United States adult population. Pooling 11 survey cycles over 24 years afforded exceptional statistical power, sufficient to detect modest nonlinear effects and subgroup differences that smaller studies would miss. Notably, we did not rely on a single modeling approach; rather, we applied three complementary nonlinear methods (RCS, GAMs, and segmented regression), each with formal statistical tests, and arrived at convergent conclusions regarding the dose–response shape. The integration of mediation and interaction analyses within the same analytical framework further distinguishes this work from prior descriptive studies.

Multicollinearity diagnostics are reported in Supplementary Table S1: the variance inflation factor (VIF) is below 2.1 for every covariate in the primary models (FPG: 1.27; AGE: 1.07; BMI: 1.50; HOMA-IR: 1.82; LOG_INSULIN: 2.09; CRP: 1.06), well below the conventional threshold of 5 used to flag problematic collinearity. This confirms that the regression coefficients are not artefactually inflated or deflated by linear dependence between predictors, and supports the side-by-side interpretation of the BMI, HOMA-IR, and CRP decomposition pathways in Figure 7.

At the same time, several limitations must be acknowledged. The cross-sectional design, while well suited for characterizing associations, precludes definitive causal inference. Our decomposition results should accordingly be interpreted as a statistical attribution of the marginal FPG–SBP association across correlated pathways rather than as confirmation of causal mediation; in particular, BMI is biologically plausible as a shared upstream confounder of both glucose and blood pressure, and the directed acyclic graph implicit in the decomposition (FPG $\rightarrow$ BMI $\rightarrow$ SBP) is one of several admissible structures. The flat slope of the FPG–SBP relationship above 122 mg/dL may also partly reflect treatment-induced bias from antihypertensive medications, which we addressed through medication-stratified segmented regression and the Tobin et al. blood-pressure correction; residual confounding from this source remains possible. Blood pressure was measured at a single visit, which may not fully represent each participant's usual ambulatory blood pressure level. The transition from auscultatory to oscillometric measurement in the 2017–2018 cycle introduces a potential methodological discontinuity, though our sensitivity analyses restricting to one measurement method at a time yielded consistent results (Table 4). Self-reported antihypertensive medication use is subject to recall bias, and unmeasured confounders—dietary sodium intake, habitual physical activity, sleep quality, and genetic predisposition among them—may contribute to residual confounding.

The GAM model achieved an adjusted R^2 of 0.225, indicating that glycemic markers, age, and BMI together explain approximately 22.5% of the variance in SBP. The substantial unexplained variance is expected given that blood pressure is determined by numerous factors not captured in this model, including genetic predisposition, dietary sodium intake, habitual physical activity, psychological stress, sleep quality, and medication effects. The

primary aim of the GAM was to characterize the shape of the dose–response relationship rather than to build a comprehensive predictive model of blood pressure.

5. Conclusions

In this large cross-sectional analysis of NHANES data spanning 24 years, we demonstrated that the relationship between fasting plasma glucose and blood pressure is significantly nonlinear, with a data-driven breakpoint at FPG = 122.1 mg/dL. Below this threshold, each 10 mg/dL increase in FPG was associated with a clinically meaningful 3.9 mmHg increase in SBP; above this threshold, the association was essentially flat. BMI accounted for approximately one-quarter of the marginal association in the statistical decomposition, while insulin resistance and inflammation did not contribute significantly as independent mediators. The glucose–BP association was stronger in females, in prediabetic individuals, and at lower BMI levels. These findings support integrated cardiometabolic risk assessment and suggest that the pre-diabetic glycemic range represents a critical window for cardiovascular risk mitigation through combined glucose and blood pressure management.

Supplementary Materials: The following supporting information can be downloaded at: https://www.mdpi.com/article/10.3390/a19050369/s1, Table S1—variance inflation factors/multicollinearity diag-nostics; Table S2—medication-stratified segmented regression by ON_BP_MEDS/ON_DM_MEDS; Table S3—breakpoint robustness across sex, age band, BMI category, and BP-measurement method; Table S4—full RCS ba-sis-term coefficients (linear, rcs1, rcs2, rcs3) for FPG-SBP and HbA1c-SBP.

Author Contributions: Conceptualization, M.K. and I.N.; data curation, I.N. and G.V.; formal analysis, M.K. and I.N.; methodology, I.N., M.K. and M.M.; software, I.N., G.V. and H.K.; validation, I.N., M.K., P.M. and H.K.; visualization, I.N. and H.K.; writing—original draft, I.N. and M.K.; writing—review and editing, M.M., G.V. and P.M. All authors have read and agreed to the published version of the manuscript.

Funding: This research received no external funding.

Institutional Review Board Statement: Not applicable. This study is a secondary analysis of publicly available, de-identified National Health and Nutrition Examination Survey (NHANES) data and does not constitute human subjects research under 45 CFR 46.

Informed Consent Statement: Not applicable. NHANES participants provided informed consent for their data to be collected and used for research purposes at the time of original data collection; the present secondary analysis used de-identified public-use files and therefore required no additional consent.

Data Availability Statement: The NHANES dataset used in this study is publicly available through the Centers for Disease Control and Prevention, National Center for Health Statistics (https://wwwn.cdc.gov/nchs/nhanes/, accessed on 14 March 2026). NHANES data are in the public domain (US government data; no restrictions on use). The analysis code is available from the corresponding author upon reasonable request.

Acknowledgments: We thank the CDC National Center for Health Statistics for making the NHANES data publicly available, and the thousands of NHANES participants who contributed their data. The presentation and dissemination of these research results are supported by National Science Fund Project КП-06-H85-7/05.12.2024 “Significance and Potential Risks of the Fast Integration of Artificial Intelligence (AI) Technologies into the Economy and Financial Sector.”.

Conflicts of Interest: The authors declare no conflicts of interest.

References

1. Mills, K.T.; Stefanescu, A.; He, J. The global epidemiology of hypertension. *Nat. Rev. Nephrol.* **2020**, *16*, 223–237. [CrossRef] [PubMed]

2. Sun, H.; Saeedi, P.; Karuranga, S.; Pinkepank, M.; Ogurtsova, K.; Duncan, B.B.; Stein, C.; Basit, A.; Chan, J.C.N.; Mbanya, J.C.; et al. IDF Diabetes Atlas: Global, regional and country-level diabetes prevalence estimates for 2021 and projections for 2045. *Diabetes Res. Clin. Pract.* **2022**, *183*, 109119. [CrossRef] [PubMed]
3. Petrie, J.R.; Guzik, T.J.; Touyz, R.M. Diabetes, Hypertension, and Cardiovascular Disease: Clinical Insights and Vascular Mechanisms. *Can. J. Cardiol.* **2018**, *34*, 575–584. [CrossRef] [PubMed]
4. de Boer, I.H.; Bangalore, S.; Benetos, A.; Davis, A.M.; Michos, E.D.; Muntner, P.; Rossing, P.; Zoungas, S.; Bakris, G. Diabetes and Hypertension: A Position Statement by the American Diabetes Association. *Diabetes Care* **2017**, *40*, 1273–1284. [CrossRef] [PubMed]
5. Lastra, G.; Dhuper, S.; Johnson, M.S.; Sowers, J.R. Salt, aldosterone, and insulin resistance: Impact on the cardiovascular system. *Nat. Rev. Cardiol.* **2010**, *7*, 577–584. [CrossRef]
6. Giacco, F.; Brownlee, M. Oxidative stress and diabetic complications. *Circ. Res.* **2010**, *107*, 1058–1070. [CrossRef] [PubMed]
7. Sowers, J.R.; Whaley-Connell, A.; Epstein, M. Narrative review: The emerging clinical implications of the role of aldosterone in the metabolic syndrome and resistant hypertension. *Ann. Intern. Med.* **2009**, *150*, 776–783. [CrossRef] [PubMed]
8. Wang, T.; Li, M.; Zeng, T.; Hu, R.; Xu, Y.; Xu, M.; Zhao, Z.; Chen, Y.; Wang, S.; Lin, H.; et al. Association Between Insulin Resistance and Cardiovascular Disease Risk Varies According to Glucose Tolerance Status: A Nationwide Prospective Cohort Study. *Diabetes Care* **2022**, *45*, 1863–1872. [CrossRef] [PubMed]
9. Barr, E.L.M.; Zimmet, P.Z.; Welborn, T.A.; Jolley, D.; Magliano, D.J.; Dunstan, D.W.; Cameron, A.J.; Dwyer, T.; Taylor, H.R.; Tonkin, A.M.; et al. Risk of cardiovascular and all-cause mortality in individuals with diabetes mellitus, impaired fasting glucose, and impaired glucose tolerance. *Circulation* **2007**, *116*, 151–157. [CrossRef] [PubMed]
10. National Center for Health Statistics. *NHANES Blood Pressure Procedures Manual*; CDC: Hyattsville, MD, USA, 2017. Available online: https://wwwn.cdc.gov/nchs/nhanes/continuousnhanes/manuals.aspx (accessed on 14 March 2026).
11. Matthews, D.R.; Hosker, J.P.; Rudenski, A.S.; Naylor, B.A.; Treacher, D.F.; Turner, R.C. Homeostasis model assessment: Insulin resistance and beta-cell function from fasting plasma glucose and insulin concentrations in man. *Diabetologia* **1985**, *28*, 412–419. [CrossRef] [PubMed]
12. Seabold, S.; Perktold, J. Statsmodels: Econometric and Statistical Modeling with Python. In Proceedings of the 9th Python in Science Conference, Austin, TX, USA, 28 June–3 July 2010; pp. 92–96. [CrossRef]
13. Virtanen, P.; Gommers, R.; Oliphant, T.E.; Haberland, M.; Reddy, T.; Cournapeau, D.; Burovski, E.; Peterson, P.; Weckesser, W.; Bright, J.; et al. SciPy 1.0: Fundamental algorithms for scientific computing in Python. *Nat. Methods* **2020**, *17*, 261–272. [CrossRef] [PubMed]
14. Servén, D.; Brummitt, C. *pyGAM: Generalized Additive Models in Python*; Zenodo: Geneva, Switzerland, 2018. [CrossRef]
15. Pedregosa, F.; Varoquaux, G.; Gramfort, A.; Michel, V.; Thirion, B.; Grisel, O.; Blondel, M.; Prettenhofer, P.; Weiss, R.; Dubourg, V.; et al. Scikit-learn: Machine Learning in Python. *J. Mach. Learn. Res.* **2011**, *12*, 2825–2830.
16. Hunter, J.D. Matplotlib: A 2D Graphics Environment. *Comput. Sci. Eng.* **2007**, *9*, 90–95. [CrossRef]
17. Johnson, C.L.; Paulose-Ram, R.; Ogden, C.L.; Carroll, M.D.; Kruszon-Moran, D.; Dohrmann, S.M.; Curtin, L.R. *National Health and Nutrition Examination Survey: Analytic Guidelines, 1999–2010*; Vital Health Stat. 2; National Center for Health Statistics: Washington, DC, USA, 2013; Volume 161, pp. 1–24.
18. Baron, R.M.; Kenny, D.A. The moderator-mediator variable distinction in social psychological research: Conceptual, strategic, and statistical considerations. *J. Pers. Soc. Psychol.* **1986**, *51*, 1173–1182. [CrossRef] [PubMed]
19. Preacher, K.J.; Hayes, A.F. Asymptotic and resampling strategies for assessing and comparing indirect effects in multiple mediator models. *Behav. Res. Methods* **2008**, *40*, 879–891. [CrossRef] [PubMed]
20. Tobin, M.D.; Sheehan, N.A.; Scurrah, K.J.; Burton, P.R. Adjusting for treatment effects in studies of quantitative traits: Antihypertensive therapy and systolic blood pressure. *Stat. Med.* **2005**, *24*, 2911–2935. [CrossRef] [PubMed]
21. Emdin, C.A.; Anderson, S.G.; Woodward, M.; Rahimi, K. Usual Blood Pressure and Risk of New-Onset Diabetes: Evidence From 4.1 Million Adults and a Meta-Analysis of Prospective Studies. *J. Am. Coll. Cardiol.* **2015**, *66*, 1552–1562. [CrossRef] [PubMed]
22. Meigs, J.B.; D'Agostino, R.B., Sr.; Wilson, P.W.F.; Cupples, L.A.; Nathan, D.M.; Singer, D.E. Risk Variable Clustering in the Insulin Resistance Syndrome: The Framingham Offspring Study. *Diabetes* **1997**, *46*, 1594–1600. [CrossRef] [PubMed]
23. Hall, J.E.; do Carmo, J.M.; da Silva, A.A.; Wang, Z.; Hall, M.E. Obesity, kidney dysfunction and hypertension: Mechanistic links. *Nat. Rev. Nephrol.* **2019**, *15*, 367–385. [CrossRef]
24. Regensteiner, J.G.; Golden, S.; Huebschmann, A.G.; Barrett-Connor, E.; Chang, A.Y.; Chyun, D.; Fox, C.S.; Kim, C.; Mehta, N.; Reckelhoff, J.F.; et al. Sex Differences in the Cardiovascular Consequences of Diabetes Mellitus: A Scientific Statement From the American Heart Association. *Circulation* **2015**, *132*, 2424–2447. [CrossRef]

Disclaimer/Publisher's Note: The statements, opinions and data contained in all publications are solely those of the individual author(s) and contributor(s) and not of MDPI and/or the editor(s). MDPI and/or the editor(s) disclaim responsibility for any injury to people or property resulting from any ideas, methods, instructions or products referred to in the content.